Numerical Investigation of Hybrid Thin-Ply Laminates for Matrix Cracking and Delamination Suppression in Linerless Cryogenic Hydrogen Tanks

P. Shabani[1*], M. Lanzo[1], L. Li[2], J. Laliberte[1]

[1] Department of Mechanical and Aerospace Engineering, Carleton University, Ottawa, Canada

[2] Aerospace Research Centre, National Research Council Canada, Ottawa, Canada

* *Corresponding author (peyman.shabani@carleton.ca)*

Keywords: *Composite materials, Aviation, Cryogenic hydrogen storage, Fatigue, Finite element analysis*

1. Abstract

Thin-ply composites have been regarded as a promising approach for suppressing matrix cracking and delamination in linerless Type V cryogenic hydrogen tanks. This study investigates ply-bridging mechanisms for retarding thermal-mechanical fatigue damage through ply-thickness hybridization in composite laminates. A progressive damage model was developed using cohesive zone modeling (CZM) and continuum damage mechanics (CDM) to predict delamination and intralaminar failure modes based on the enhanced LaRC05 failure criteria. The model was implemented via a user-defined material subroutine in the Abaqus finite element analysis software. Temperature-dependent fracture toughness and elastic moduli were incorporated to account for matrix embrittlement at cryogenic temperatures. The model's capability to predict leakage was first validated against existing experimental results for T700SC/2500 at room temperature. Subsequently, the model was applied to IM7/977-2 at both room and cryogenic temperatures to investigate the effect of ply hybridization on gas leakage. The results indicate that hybrid architectures incorporating thin plies can delay the onset of transverse microcracking and prevent the coalescence of cracks into through-thickness leakage paths. These findings demonstrate that hybrid thin-ply laminates can enhance structural integrity and improve resistance to gas permeation.

2. Introduction

The development of lightweight cryogenic liquid hydrogen storage solutions is critical to decarbonizing air transport. While carbon fiber-reinforced polymer composites offer high specific strength, they remain susceptible to microcracking and delamination induced by extreme temperature variations during cryogenic tank operations [1]. It has been reported that reducing ply thickness, while maintaining the overall laminate thickness, decreases the energy release rate at the crack tip [2]. This reduction can effectively delay the onset of transverse matrix cracks during thermal cycling. In addition, thin-ply laminates have been shown to exhibit a higher damage tolerance compared with conventional ones [3–5].

Gas leakage in composite storage has been studied numerically [6–8]. The influence of the stacking sequence on gas permeability has also been investigated [9,10]. It has been reported that under multiaxial loading conditions, matrix damage evolves from dispersed matrix cracks into multilayer intersecting cracks that can create through-thickness pathways for gas leakage. Although a metal or polymer liner can prevent the leakage [11], these liners are not weight-efficient, and thus it is desirable for the composite material itself to act as a barrier. Most published literature on gas leakage simulation focuses primarily on room temperature conditions. However, since liquid hydrogen tanks must operate under cryogenic conditions, it is necessary to investigate the performance of composite hydrogen tanks at cryogenic temperatures as well.

The current study focuses on the use of thin-ply composites as leakage barriers in hydrogen tanks. While thin-ply composites may offer improved damage resistance, they can increase manufacturing time and costs due to the greater number of plies required for layup. This study aims to numerically evaluate the strains corresponding to the onset of leakage in four laminate configurations with similar total thicknesses but different proportions of thin plies, under both room temperature and cryogenic conditions.

3. Finite element analysis

3.1. Finite element model

To predict the onset of gas leakage, a 1 mm × 1 mm idealized unit cell of a composite was modeled in Abaqus. Within each ply of the unit cell, a predefined crack path was introduced using cohesive elements. Additionally, a cohesive layer was inserted between adjacent plies with different fiber orientations to model delamination, as schematically shown in Figure 1. It was assumed that leakage initiates once matrix cracking occurs in all plies, accompanied by damage to the interlaminar cohesive layers, thereby forming a continuous through-thickness pathway for gas leakage.

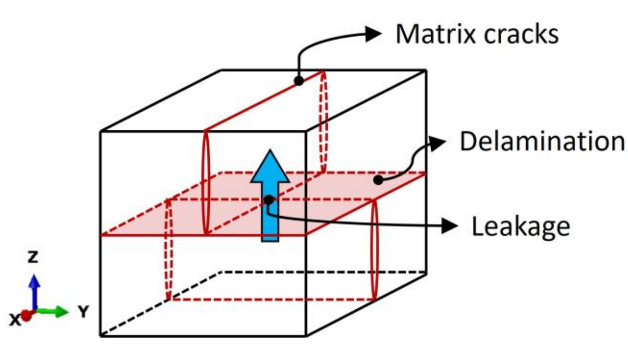

Figure 1. A schematic of gas leakage induced by the connection of matrix cracks.

The Abaqus/explicit was used for the simulation. To accelerate the computational time, a mass scaling technique was applied with a target minimum stable time increment (STI) of 2×10^{-5}. With this mini STI, the kinetic energy remained below 5% of the internal energy throughout the simulation. The total step time was set to 1. Biaxial loading of equal magnitude was applied in both the X and Y directions (Figure 1). Periodic boundary conditions were enforced on the unit cell faces [12]. To further improve computational efficiency, only half of the laminate thickness was modeled, with a symmetry boundary condition applied to the bottom surface of the unit cell.

To validate the model, available experimental results [19] for the leakage rate of T700SC/2500 at room temperature were used for Layup A and Layup B, as shown in Figure 2. The thickness of each ply was 0.06 mm. Additionally, Layup C and Layup D were modeled to compare their strain at leakage onset. In Figure 2, the red regions between and within the plies are cohesive element zones.

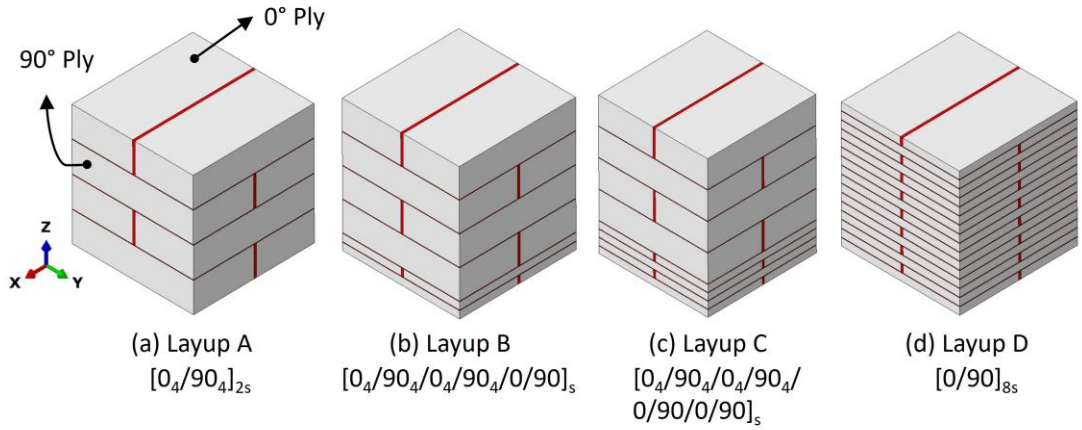

Figure 2. Finite element models used for validation (T700SC/2500).

After validating the model, the same modeling approach was applied to IM7/977-2 with the four layups shown in Figure 3. This second material system was selected because the cryogenic mechanical properties of T700SC/2500 were unavailable in the literature. The ply thickness of IM7/977-2 was 0.12 mm. Layups 1, 3, and 4 had an identical total thickness of 1.92 mm, while the thickness of Layup 2 was 2.4 mm. The element size was specified as 0.025 mm × 0.025 mm × 0.025 mm using a global seed size of 0.025 mm in Abaqus. In the continuum and cohesive regions, C3D8R and COH3D8 elements were used, respectively.

The material properties utilized for both T700SC/2500 and IM7/977-2 are provided in Table 1. The ply interface properties used for the cohesive zone modeling (CZM) are provided in Table 2. For IM7/977-2 at cryogenic temperature, only the mode I fracture toughness (G_{IC}) was available. Consequently, it was assumed in this study that the Mode II and Mode III fracture toughness values (G_{IIC} and G_{IIIC}) decrease at a rate similar to that of G_{IC}.

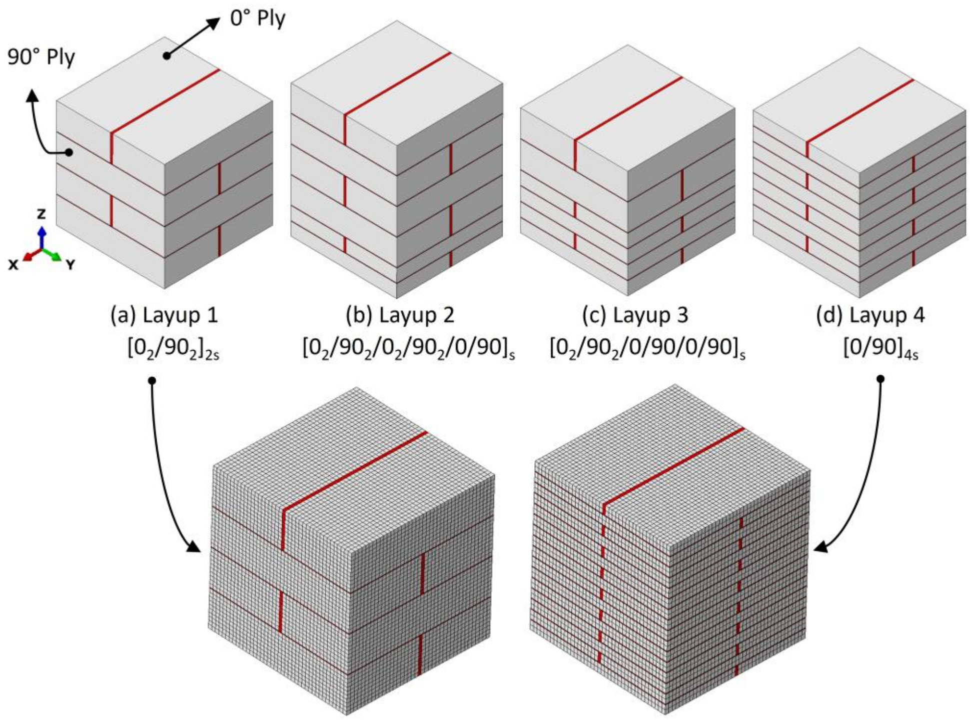

Figure 3. Finite element models (IM7/977-2).

Table 1. Mechanical properties of T700SC/2500 and IM7/977-2.

	T700SC/2500		IM7/977-2		
Property	Room Temp. (293 K)	Ref.	Room Temp. (293 K)	Cryogenic (20 K)	Ref.
Tensile longitudinal modulus, E_{1T}^{0} (GPa)	133	[13]	160	143	[14]
Compressive longitudinal modulus, E_{1C}^{0} (GPa)	133	[13]	148	140	[14]
Transverse modulus, E_2 (GPa)	9.1	[13]	9.3	19.3	[14]
Out-of-plane modulus, E_3 (GPa)	9.1	[13]	9.3	19.3	[14]
In-plane shear modulus, G_{12} (GPa)	5.67	[13]	5.16	7.99	[14]
Inter-laminar shear modulus, G_{13} (GPa)	5.67	[13]	5.16	7.99	[14]
Inter-laminar shear modulus, G_{23} (GPa)	3.5	[13]	3.14	3.14	[14]
In-plane Poisson’s ratio, ν_{12}	0.31	[13]	0.3	0.3	[14]
Inter-laminar Poisson’s ratio, ν_{13}	0.31	[13]	0.3	0.3	[14]
Inter-laminar Poisson’s ratio, ν_{23}	0.46	[15]	0.46	0.46	[16]
Longitudinal tensile strength, X_T (MPa)	2507	[13]	2953	2953	[17]
Longitudinal compressive strength, X_C (MPa)	1201	[13]	1447	1447	[17]
Transverse tensile strength, Y_T (MPa)	61.8	[13]	72	82	[17]
Transverse compressive strength, Y_C (MPa)	186	[13]	200	200	[18]
In-plane shear strength, S_L (MPa)	84.8	[13]	126	141	[17]
Interlaminar shear strength, S_T (MPa)	41.6	[13]	104	104	[16]

	T700SC/2500		IM7/977-2		
Property	Room Temp. (293 K)	Ref.	Room Temp. (293 K)	Cryogenic (20 K)	Ref.
Longitudinal tensile failure strain, ε_{1T} (%)	1.88	-	1.85	2.07	-
Longitudinal compressive failure strain, ε_{1C} (%)	0.90	-	0.98	1.03	-
Transverse tensile failure strain, $\varepsilon^{f}{}_{2T}$ (%)	0.68	-	0.77	0.42	-
Transverse compressive failure strain, $\varepsilon^{f}{}_{2C}$ (%)	2.04	-	2.15	1.04	-
In-plane shear failure strain, $\varepsilon^{f}{}_{12}$ (%)	1.50	-	2.44	1.76	-
Inter-laminar shear failure strain, $\varepsilon^{f}{}_{13}$ (%)	0.73	-	2.01	1.30	-
Inter-laminar shear failure strain, $\varepsilon^{f}{}_{23}$ (%)	1.19	-	3.31	3.31	-

Table 2. Ply interface properties used for T700SC/2500 and IM7/977-2.

	T700SC/2500		IM7/977-2		
Property	Room Temp. (293 K)	Ref.	Room Temp.	Cryogenic (83 K)	Ref.
Penalty stiffness, K^0 (N/mm^3)	5×10^{6} *	-	5×10^{6} *	5×10^{6} *	-
Mode-I maximum traction, T_n (MPa)	60	[19]	60	60	-
Mode-II maximum traction, T_s (MPa)	80	[19]	80	80	-
Mode-III maximum traction, T_t (MPa)	80	[19]	80	80	-
Mode-I fracture toughness, G_{IC} (N/mm)	0.4	[19]	0.31	0.26	[20]
Mode-II fracture toughness, G_{IIC} (N/mm)	0.8	[19]	1.68	1.41†	[21]
Mode-III fracture toughness, G_{IIIC} (N/mm)	0.8	[19]	1.68	1.41†	[21]
B-K Mixed-mode Parameter, η	2.28	[19]	1.39	1.39	[21]

* The same value was used for the penalty stiffness for all three fracture modes I, II, and III.
† G_{IC} at cryogenic temperature (83 K) has been reported in [20]. It was assumed that G_{IIC} and G_{IIIC} decrease at a rate similar to that of G_{IC}.

3.2. Modeling of matrix cracking, delamination, and fiber failures

Matrix cracking and delamination were modeled using the CZM technique based on a bilinear traction-separation law. Damage onset under mixed-mode loading was determined using the quadratic stress criterion [16], and damage propagation was governed by the "Benzeggagh-Kenane (B-K)" damage criterion [21].

The fiber breakage, fiber splitting, and fiber kinking failure modes were captured using a vectorized user-defined material (VUMAT) subroutine developed based on the enhanced LaRC05 failure criteria [16]. The details regarding these failure criteria can be found in [16].

4. Results and discussions

4.1. Model validation

The experimental leakage rates of biaxially loaded T700SC/2500 specimens with Layups A and B (shown in Figure 2) were reported by Hamori *et al.* [19] and are illustrated in Figure 4. To measure the leakage rates at different strain levels, the applied strain was increased incrementally over 18 cycles. For Layups A and B, the leakage was observed at strains of 0.79% and 0.99%, respectively. The present model predicted the leakage strain for Layup A with a 14% underestimation and for Layup B with a 21% overestimation. One of the main sources of these discrepancies lies in the CZM parameters used in the simulation. In the current study, the properties provided in [19] were used; however, the reported fracture toughness in that study was rounded and may lack high experimental precision.

In addition to Layups A and B, two additional configurations with a higher proportion of thin plies were modeled. Layup C contained eight thin plies, and Layup D was made entirely of thin plies. The predicted leakage strains for all configurations are shown in Figure 4. An interesting finding of this study was that the leakage strain for Layup C was comparable to that of Layup D. This suggests that a hybrid laminate incorporating only a limited number of thin plies can achieve damage tolerance comparable to that of a full thin-ply laminate, which typically requires greater manufacturing time and cost. It should be noted that in this section, "thin-ply" refers to a single ply of 0.06 mm thickness, and the thicker plies consisted of many plies each with a thickness of 0.06 mm. Compared with Layup A without any thin ply, the leakage biaxial strains (ε_x *and* ε_y) for Layups B, C, and D increased by 76%, 126%, and 138%, respectively. The strains were obtained by dividing the global displacements in the X and Y directions by the height and width of the unit cell (1 mm).

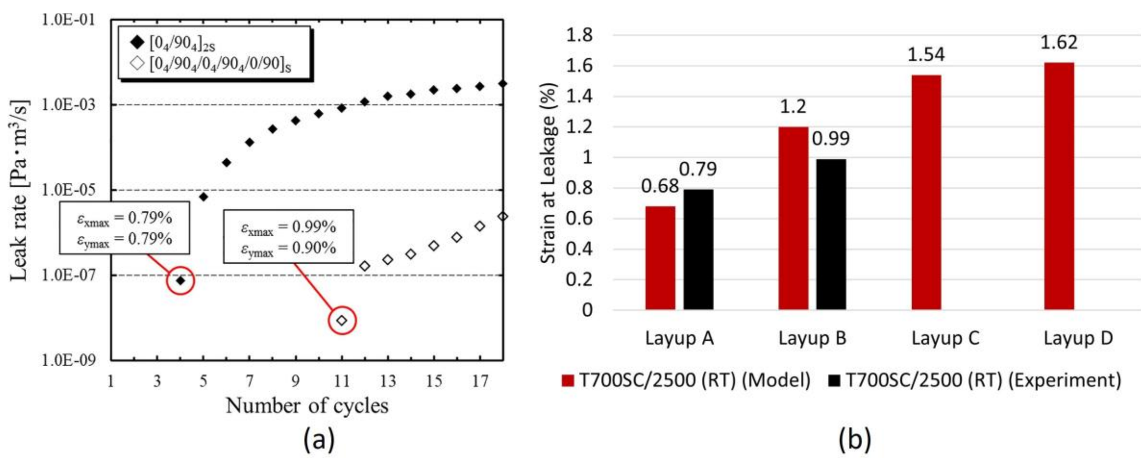

Figure 4. (a) Leakage rates for Layup A and Layup B [19]. *(b) Comparison of model predictions and experimental results for strain at leakage.*

4.2. FEA results

Following model validation, the same modeling approach was applied to IM7/977-2 at both room and cryogenic temperatures. Four layups with different proportions of thin plies were evaluated. The resulting damaged states for Layups 1 and 2 are shown in Figure 5, and for Layups 3 and 4 are shown in Figure 6. For each case, the first row illustrates the inter- and intralaminar cohesive elements at three distinct strain levels corresponding to the onset of matrix cracking, delamination, and gas leakage, respectively. In these contours, the colors represent the damage variable, where elements were deleted upon reaching a damage threshold of 0.99. The CZM damage parameters were obtained directly from the scalar degradation parameter (SDEG) in Abaqus. The second row displays the fiber failure index contours at the leakage onset strain. The leakage happens when matrix cracks connect and create a path for gas through the thickness of the laminate. It was predicted that no fiber failure would happen before the start of the leakage in any of the cases.

The results are summarized in Figure 7 and Table 3. Overall, the strains corresponding to the onset of matrix cracking, delamination, and gas leakage were lower under cryogenic conditions. On average, the leakage strain at the cryogenic temperature was 30% lower than at room temperature. The initiation strains for matrix cracking and delamination were similar for Layups 1, 2, and 3, because these damage mechanisms initiated at nearly identical strain levels within the thicker plies. However, the presence of thin plies in Layups 2 and 3 delayed leakage initiation due to the higher strains required to induce matrix cracking and delamination in thin-ply blocks. Since the loading is biaxial, and periodic boundary conditions are applied, edge effects cannot cause delamination. However, delamination can be caused by crack-induced interlaminar stress concentrations at the intersections where the matrix cracks meet the adjacent ply interfaces. Relative to Layup 1, the room-temperature leakage strain increased by 41%, 54%, and 129% for Layups 2, 3, and 4, respectively, while the corresponding improvements under cryogenic conditions were 19%, 36%, and 100%. Comparing IM7/977-2 (0.12 mm ply thickness) with T700SC/2500 (0.06 mm ply thickness), it can be concluded that thinner plies provide a more pronounced improvement in resistance to hydrogen leakage.

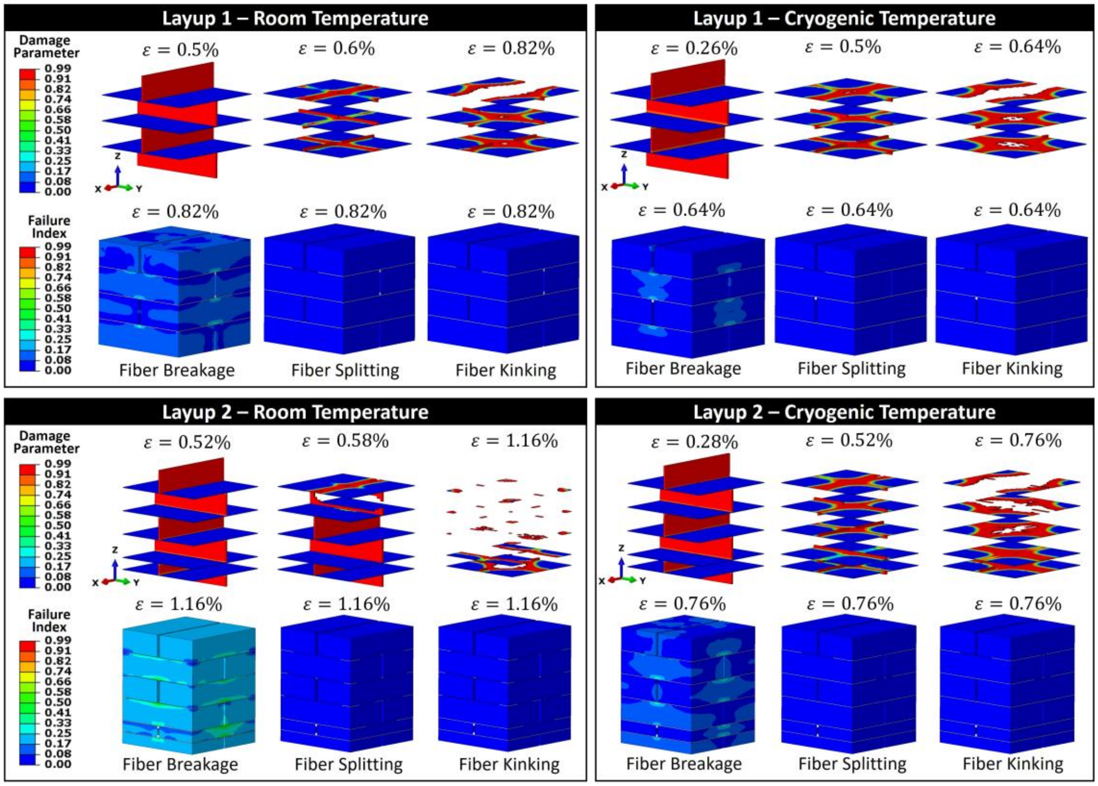

Figure 5. Damage progression comparison at room and cryogenic temperatures for Layup 1 and Layup 2.

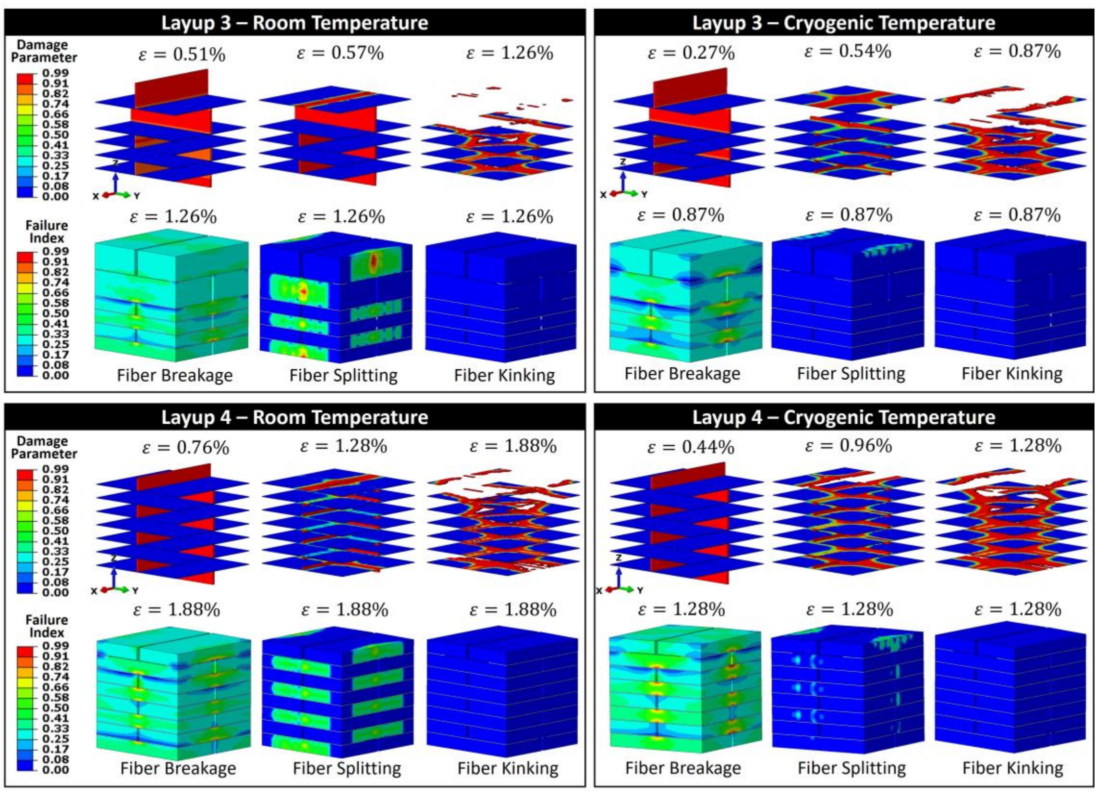

Figure 6. Damage progression comparison at room and cryogenic temperatures for Layup 3 and Layup 4.

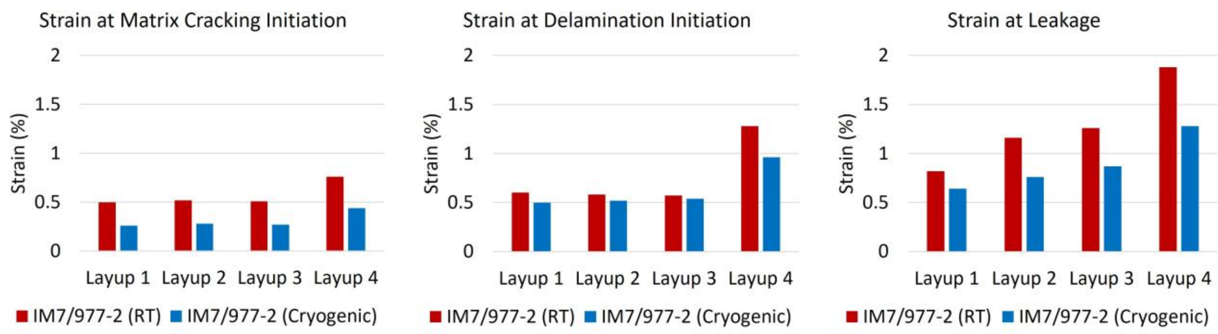

Figure 7. Comparison of strains at matrix cracking initiation, delamination initiation, and start of leakage at room and cryogenic temperatures.

Table 3. Strains at matrix cracking initiation, delamination initiation, and start of leakage at room and cryogenic temperatures.

	Biaxial strain at matrix cracking initiation (%)		Biaxial strain at delamination initiation (%)		Biaxial strain at leakage (%)	
	RT	Cryogenic	RT	Cryogenic	RT	Cryogenic
Layup 1	0.5	0.26	0.6	0.5	0.82	0.64
Layup 2	0.52	0.28	0.58	0.52	1.16	0.76
Layup 3	0.51	0.27	0.57	0.54	1.26	0.87
Layup 4	0.76	0.44	1.28	0.96	1.88	1.28

5. Conclusions

This study successfully demonstrated through high-fidelity simulations that hybrid thin-ply laminate architectures can effectively suppress matrix cracking and delamination, thereby preventing the formation of connected through-thickness gas leakage pathways in linerless cryogenic hydrogen tanks. Through finite element analysis using a progressive damage model, it was shown that cryogenic conditions reduce the allowable strain at leakage by an average of 30% compared to room temperature. Nevertheless, the incorporation of thin plies significantly enhances damage tolerance under both room temperature and cryogenic conditions. Notably, hybrid laminates containing only a small fraction of thin plies (approximately 20% of the laminate volume) achieved leakage strain improvements nearly comparable to the laminates constructed entirely of thin plies. This finding indicates that strategic ply-thickness hybridization offers an efficient and cost-effective manufacturing approach for maintaining structural integrity and improving gas impermeability of composite hydrogen storage.

6. References

[1] Grogan DM, Brádaigh CMÓ, McGarry JP, Leen SB. Damage and permeability in tape-laid thermoplastic composite cryogenic tanks. Compos Part A Appl Sci Manuf 2015;78:390–402.

[2] Teixeira RF, Pinho ST, Robinson P. Thickness-dependence of the translaminar fracture toughness: experimental study using thin-ply composites. Compos Part A Appl Sci Manuf 2016;90:33–44.

[3] Sihn S, Kim RY, Kawabe K, Tsai SW. Experimental studies of thin-ply laminated composites. Compos Sci Technol 2007;67:996–1008.
[4] Yokozeki T, Aoki Y, Ogasawara T. Experimental characterization of strength and damage resistance properties of thin-ply carbon fiber/toughened epoxy laminates. Compos Struct 2008;82:382–9.
[5] Yokozeki T, Kuroda A, Yoshimura A, Ogasawara T, Aoki T. Damage characterization in thin-ply composite laminates under out-of-plane transverse loadings. Compos Struct 2010;93:49–57.
[6] Kumazawa H, Whitcomb J. Numerical modeling of gas leakage through damaged composite laminates. J Compos Mater 2008;42:1619–38.
[7] Xu J, Sankar B V. Prediction of stitch crack evolution and gas permeability in multidirectional composite laminates. Compos Part A Appl Sci Manuf 2008;39:1625–31.
[8] Xu J, Sankar B V, Bapanapalli S. Finite element based method to predict gas permeability in cross-ply laminates. J Compos Mater 2008;42:849–64.
[9] Kumazawa H, Aoki T, Susuki I. Influence of stacking sequence on leakage characteristics through CFRP composite laminates. Compos Sci Technol 2006;66:2107–15.
[10] Kumazawa H, Hayashi H, Susuki I, Utsunomiya T. Damage and permeability evolution in CFRP cross-ply laminates. Compos Struct 2006;76:73–81.
[11] Higuchi K, Takeuchi S, Sato E, Naruo Y, Inatani Y, Namiki F, et al. Development and flight test of metal-lined CFRP cryogenic tank for reusable rocket. Acta Astronaut 2005;57:432–7.
[12] Tian W, Qi L, Chao X, Liang J, Fu M. Periodic boundary condition and its numerical implementation algorithm for the evaluation of effective mechanical properties of the composites with complicated micro-structures. Compos Part B Eng 2019;162:1–10.
[13] Wang Y, Liu T, Jiang P. Experimental and FEM studies on secondary co-curing reinforcement of laminates. Materials (Basel) 2018;11:2581.
[14] Arnold SM, Bednarcyk BA, Collier CS, Yarrington PW. Spherical Cryogenic Hydrogen Tank Preliminary Design Trade Studies. 2007.
[15] Hu J, Deng X, Zhang X, Wang W-X, Matsubara T. Effect of off-axis ply on tensile properties of [0/θ] ns thin ply laminates by experiments and numerical method. Polymers (Basel) 2021;13:1809.
[16] Shabani P, Li L, Laliberte J, Qi G. Enhanced LaRC05 failure criteria for investigating low-velocity impact on fiber-reinforced composites: an experimental and computational study. Aerosp Sci Technol 2024:109554.
[17] Ju J, Pickle BD, Morgan RJ, Reddy JN. An initial and progressive failure analysis for cryogenic composite fuel tank design. J Compos Mater 2007;41:2545–68.
[18] Acanfora V, Baldieri F, Garofano A, Fittipaldi F, Riccio A. On the crashworthiness behaviour of innovative sandwich shock absorbers. Polymers (Basel) 2022;14:4163.
[19] Hamori H, Kumazawa H, Higuchi R, Yokozeki T. Numerical and experimental evaluation of the formation of leakage paths through CFRP cross-ply laminates with leak barrier layers. Compos Struct 2019;230:111530.
[20] Johnson WS, Pavlick MM, Oliver MS. Determination of interlaminar toughness of IM7/977-2 composites at temperature extremes and different thicknesses 2005.
[21] Reeder JR. 3-D mixed mode delamination fracture criteria-An experimentalist's perspective. Am. Soc. Compos. 21st Annu. Tech. Conf., 2006.